Int. J. Heat Mass Transfer. Vol. 16, pp. 1477–1487. Pergamon Press 1973. Printed in Great Britain

THERMAL RADIATIVE PROPERTIES OF A SMOOTH AIR–WATER INTERFACE*

B. F. ARMALY, A. L. CROSBIE, D. C. LOOK and H. F. NELSON

Thermal Radiative Transfer Group, Department of Mechanical and Aerospace Engineering, University of Missouri–Rolla, Rolla, Missouri, U.S.A.

(*Received* 22 *May* 1972 *and in revised form* 7 *December* 1972)

Abstract—Thermal radiative properties for an air–water interface were calculated by considering the interface to be smooth and the water to be at uniform temperature. Monochromatic hemispherical and total normal reflectance, monochromatic and total normal transmittance, Planck mean and Rosseland mean absorption coefficients were evaluated. The wavelength interval covered by the calculations was between 0·2 and 200 μ. Other thermal radiative properties, such as emittance and absorptance, were related to the above properties, and a comparison with available results shows favorable agreement. The use of these properties in the area of remote sensing and global energy balance makes the data essential for identifying the most effective region of the spectrum and for explaining some of the naturally occurring processes where radiative transfer plays an important role.

NOMENCLATURE

$E_{b\lambda}(T)$, Planck function;
k_λ, imaginary part of refractive index at λ;
n_λ, real part of refractive index at λ;
T_s, source temperature;
T_w, water temperature;
s, path length;
x, depth;
cm, centimeters;
m, meters;
km, kilometers;
$\alpha_\lambda(s)$, spectral absorptance at s;
$\alpha_n(x)$, total absorptance for normal incidence at x;
$\alpha_n(T_s)$, total normal absorptance;
$\alpha(T_s)$, total hemispherical absorptance;
ϵ_λ, monochromatic hemispherical emittance,;
$\epsilon_\lambda(\theta)$, monochromatic directional emittance;
$\epsilon(T_w)$, total hemispherical emittance;
θ, incident polar angle;
κ_λ, spectral absorption coefficient;
κ_p, Planck mean absorption coefficient;
κ_R, Rosseland mean absorption coefficient;
κ_m, mean absorption coefficient;
λ, wavelength;
μ, microns;
$\rho_{\perp\lambda}(\theta)$, perpendicularly polarized reflectance component;
$\rho_{\parallel\lambda}(\theta)$, parallel polarized reflectance component;
$\rho_\lambda(\theta)$, monochromatic specular reflectance;
$\rho_{H\lambda}$, monochromatic hemispherical reflectance;
$\rho_{n_\lambda}(\theta)$, monochromatic normal reflectance;
σ, Stefan–Boltzmann constant;
τ, transmittance;
$\tau_\lambda(s)$, spectral transmittance at s;
$\tau_n(x)$, total transmittance for normal incidence at x;
Φ, polar angle in the medium.

INTRODUCTION

WATER temperature at different depths below the surface is governed in part by the intensity

* Work supported in part by the National Science Foundation under grant numbers GK-32679 and GK-5238.

of transmitted radiant energy and in part by the emission and absorption characteristics of the water. Because subaqueous plants and animals are partially dependent on the solar energy transmitted through the air–water interface, marine biologists and physicists have measured the transmission and absorption characteristics of ocean and lake waters for the transmitted portion of the solar irradiation [1–4]. Their studies, however, have been limited to the visible part of the spectrum where the photosynthetic mechanism and water weed respiration rates are active [5].

The reflective properties of water in the infrared play an important role in the field of remote sensing and thermal energy transfer (global energy balance) [6–8], but there is little information in the engineering literature on the thermal radiative properties of water.

Existing definitions and procedures, commonly used in thermal radiative transfer studies, have been used to calculate and examine the thermal radiative properties of an air–water interface over a wide region of the spectrum. Even though the present model is oversimplified, it serves as a preliminary step for calculation.

The real, n_λ, and the imaginary, k_λ, parts of the complex index of refraction for distilled water have been experimentally determined over a wide region of the spectrum. Irvine and Pollack [9], Davis [10], and Zolotarev *et al.* [11] have reviewed in detail the literature in which n_λ and k_λ have been discussed. Few actual calculations have been made on the radiative transfer through water or on the radiative properties which play an important role in such a process, such as absorptivity, emissivity, and transmissivity. Mikhaylov and Zolotarev [12] calculated the monochromatic normal emittance of distilled water in the infrared, and Hyatt [13] reported its values in the microwave region. Tyler and Smith [14] made numerous experimental measurements of solar transmittance through ocean and lake waters. In the present study, we have extended our calculations to cover a larger region of the spectrum and include listings of some important radiative properties.

THEORY

We have used a simplified model to simulate an actual air–water interface. This model assumes that the air–water interface is smooth and that the water occupies the lower semi-infinite region and the air the upper semi-infinite region (Fig. 1). Collimated electromagnetic radiation incident on the interface from the direction of the air is either reflected or refracted and eventually absorbed by the water

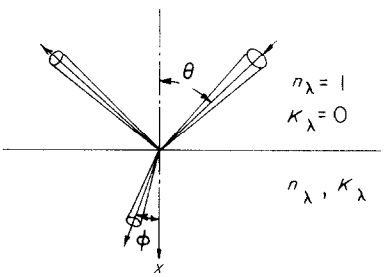

FIG. 1. Air–water interface model geometry.

with no scattering. The real and imaginary parts of the complex index of refraction for air are taken as unity and zero, respectively. The water and air temperatures, T_w, are assumed to be equal and uniform at 300°K, while the solar source temperature, T_s, is assumed to be 6000°K. Local thermodynamic equilibrium was assumed to exist thus permitting the application of Kirchhoff's law on a spectral basis.

Spectral properties

For a given wavelength, λ, and angle of incidence, θ, where the real, n_λ, and the imaginary, k_λ, parts of the index of refraction for water are known, the Fresnel relations are used to calculate the specular reflectances at the interface [15]. These relations can be summarized as follows:

$$\rho_{\perp\lambda}(\theta) = \frac{a^2 + b^2 - 2a\cos\theta + \cos^2\theta}{a^2 + b^2 + 2a\cos\theta + \cos^2\theta} \quad (1)$$

and

$$\rho_{\parallel\lambda}(\theta) = \rho_{\perp\lambda}(\theta) \left[\frac{a^2 + b^2 - 2a\sin\theta\tan\theta + \sin^2\theta\tan^2\theta}{a^2 + b^2 + 2a\sin\theta\tan\theta + \sin^2\theta\tan^2\theta}\right], \quad (2)$$

where

$$2a^2 = [(n^2 - k^2 - \sin^2\theta)^2 + 4n^2k^2]^{0.5} + (n^2 - k^2 - \sin^2\theta)$$

$$2b^2 = [(n^2 - k^2 - \sin^2\theta)^2 + 4n^2k^2]^{0.5} - (n^2 - k^2 - \sin^2\theta)$$

and where $\rho_{\perp\lambda}(\theta)$ and $\rho_{\parallel\lambda}(\theta)$ are the perpendicular and parallel polarized components of the reflectance respectively.

When the incident radiation is uniformly polarized, the monochromatic specular reflectance becomes the average of the two components and is given by

$$\rho_\lambda(\theta) = \tfrac{1}{2}[\rho_{\perp\lambda}(\theta) + \rho_{\parallel\lambda}(\theta)]. \quad (3)$$

By using Kirchoff's law and the fact that the water occupies the lower semi-infinite region (the water is of infinite depth) the monochromatic directional emittance can be calculated by using

$$\epsilon_\lambda(\theta) = 1 - \rho_\lambda(\theta). \quad (4)$$

The monochromatic hemispherical emittance, ϵ_λ, can be calculated by using the following definition:

$$\epsilon_\lambda = 2\int_0^{\pi/2} \epsilon_\lambda(\theta)\cos\theta\sin\theta\,d\theta \quad (5)$$

and the monochromatic hemispherical reflectance is defined as $\rho_{H\lambda} = 1 - \epsilon_\lambda$. The integral in equation (5) is evaluated numerically with a seventh order Gaussian quadrature.

Total properties

For some applications, such as a global energy balance, the radiative transfer from the water can be considered strictly as a surface phenomenon. For these applications, total properties are useful. The total normal absorptance, α_n, and total hemispherical absorptance, α, for a black body source at T_s are calculated by using

$$\alpha_n(T_s) = \frac{\int_0^\infty \epsilon_\lambda(0)\,E_{b\lambda}(T_s)\,d\lambda}{\sigma T_s^4} \quad (6)$$

and

$$\alpha(T_s) = \frac{\int_0^\infty \epsilon_\lambda E_{b\lambda}(T_s)\,d\lambda}{\sigma T_s^4}, \quad (7)$$

where $E_{b\lambda}(T_s)$ is the Planck function. The total hemispherical emittance is calculated at the water temperature, T_w, by

$$\epsilon(T_w) = \frac{\int_0^\infty \epsilon_\lambda E_{b\lambda}(T_w)\,d\lambda}{\sigma T_w^4}. \quad (8)$$

The integrals in equations (6)–(8) are evaluated by using the trapezoidal rule. The parameter α_n/ϵ is frequently used in heat transfer calculations involving solar radiation.

It should be noted that radiant energy received by a body of water in nature does not possess the spectral distribution of a blackbody. Atmospheric conditions modify significantly the magnitude and the spectral distribution of that incident energy and thus effect the total properties. The model of black body incident radiation, used in this study, should give the proper trends and approximate magnitudes for these properties.

Planck and Rosseland means

The gray approximation is often employed to simplify the calculation of radiative transfer through water. The gray approximation replaces the spectral absorption coefficient by a mean absorption coefficient which is independent of frequency. The Planck and Rosseland means, the most commonly used, are thus

considered here and are defined as

$$\kappa_p = \frac{\int_0^\infty \kappa_\lambda n_\lambda^2 E_{b\lambda}(T_w)\,d\lambda}{\int_0^\infty n_\lambda^2 E_{b\lambda}(T_w)\,d\lambda} \quad (9)$$

and

$$\frac{1}{\kappa_R} = \frac{\int_0^\infty \frac{n_\lambda^2}{\kappa_\lambda}\frac{dE_{b\lambda}}{dT}\,d\lambda}{\int_0^\infty n_\lambda^2 \frac{dE_{b\lambda}}{dT}\,d\lambda} \quad (10)$$

where the absorption coefficient and the complex part of the index of refraction are related as follows

$$\kappa_\lambda = \frac{4\pi\kappa_\lambda}{\lambda}. \quad (11)$$

The Plank mean is usually considered useful for optically thin situations, while the Rosseland mean is used for optically thick situations. Using a mean absorption coefficient, κ_m, the transmittance at a depth, x, could be approximated by

$$\gamma = e^{-\kappa_m x/\cos\Phi}. \quad (12)$$

It should be noted that κ_m may be the Planck, Rosseland, or any other mean absorption coefficient. Φ is the angle, measured from the normal, of penetration within the media and is related to the incidence angle θ by Snell's refraction law.

Variation of absorptance and transmittance with depth

The spectral absorptance and transmittance at a depth x are defined as

$$\alpha_\lambda(s) = 1 - e^{-\kappa_\lambda s} \quad (13)$$

and

$$\tau_\lambda(s) = e^{-\kappa_\lambda s} \quad (14)$$

where $s = x/\cos\Phi$. The total absorptance and total transmittance for the normal incidence are

$$\alpha_n(x) = \frac{\int_0^\infty [1-\rho_\lambda(0)][1-e^{-\kappa_\lambda x}]\,E_{b\lambda}(T_s)\,d\lambda}{\int_0^\infty [1-\rho_\lambda(0)]E_{b\lambda}(T_s)\,d\lambda} \quad (15)$$

and

$$\tau_n(x) = \frac{\int_0^\infty [1-\rho_\lambda(0)]\,e^{-\kappa_\lambda x}E_{b\lambda}(T_s)\,d\lambda}{\int_0^\infty [1-\rho_\lambda(0)]E_{b\lambda}(T_s)\,d\lambda} \quad (16)$$

where T_s is the temperature of the source.

RESULTS AND DISCUSSION

The optical properties, n_λ and k_λ, for water are presented in Figs. 2 and 3 respectively for the spectral range from 0·2 to 200 μ. It is evident from the figures that the thermal radiation properties of water are strongly dependent on wavelength. The absorption coefficient, κ_λ, is presented in Fig. 4 and exhibits nearly the same behavior as the imaginary part of the index of refraction. A change of eight orders of magnitude

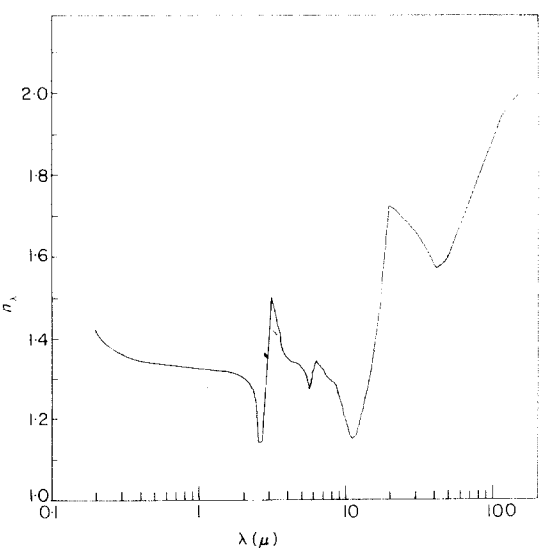

FIG. 2. Real portion of the complex index of refraction of water.

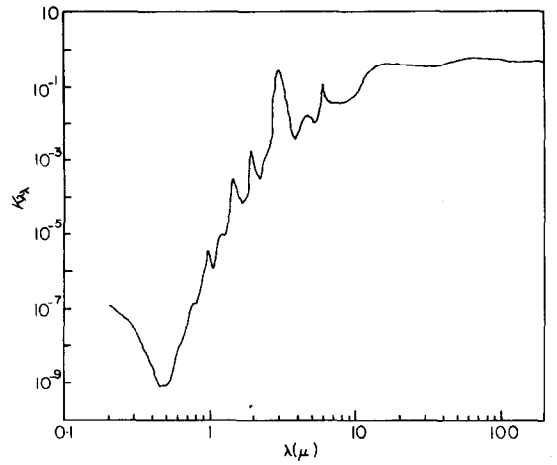

FIG. 3. Imaginary portion of the complex index of refraction of water.

in the absorption coefficient takes place between 0·45 and 4 μ with a minimum of 2×10^{-4} cm^{-1} at 0·47 μ. This feature allows solar energy in the visible portion of the spectrum, which is the driving potential for plant and animal life, to penetrate to great depths below the water surface. Thus the water layer behaves approximately as an opaque layer in the infrared and as a transparent layer in the visible.

Monochromatic reflectance

In Figs. 5 and 6, the perpendicular and parallel

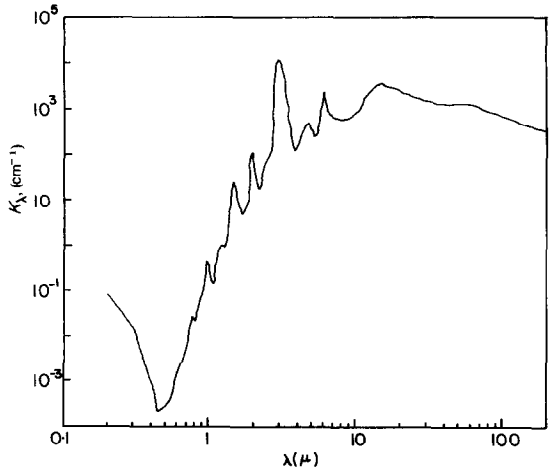

FIG. 4. Absorption coefficient.

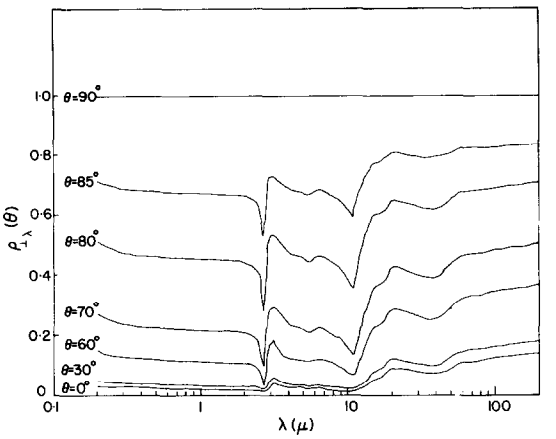

FIG. 5. Monochromatic perpendicularly polarized reflectance component for various angles of incidence.

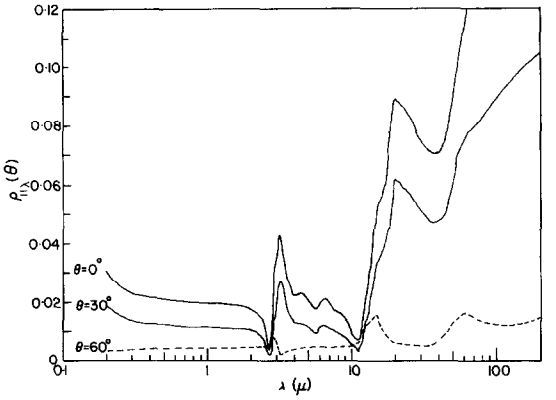

FIG. 6(a). Monochromatic parallel polarized reflectance component for various angles of incidence (reflectance decreases with angle).

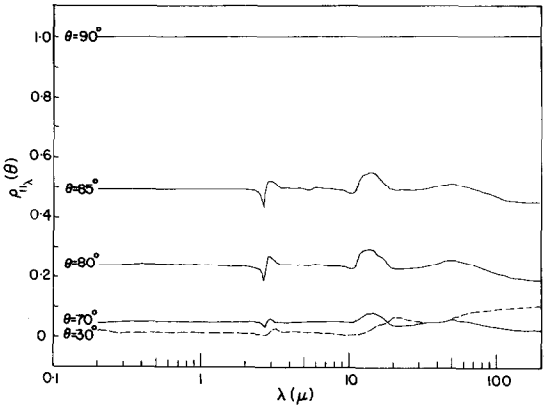

FIG. 6(b). Monochromatic parallel polarized reflectance component for various angles of incidence (reflectance increases with angle).

components of the monochromatic specular reflection are presented for different angles of incidence. The perpendicular component increases continuously as the angle of incidence increases, while the parallel component decreases first and then increases rapidly for incidence angles in the neighborhood of 90 degrees. The parallel component is a minimum at the pseudo-Brester angle, $\theta \simeq 53{\cdot}2$ degrees and a wavelength of 0·5 μ. At large angles of incidence, $\theta > 70$ degrees, the spectral variation of the parallel component is much less than the spectral variation of the perpendicular component. Both components of reflectance are relatively small except at large angles of incidence. The two components are equal when the angle of incidence is zero or 90 degrees. For remote sensing or spectral identification, the difference between the two polarized components can be quite significant.

In the visible region of the spectrum, the reflectance is constant, while in the infrared the reflectance changes significantly. For example, the reflectance for normal incidence varies over an order of magnitude from 10 to 20 μ. There are also large variations near 3 μ. As expected, the spectral variations of the reflectance are similar to the spectral variation of the index of refraction; however, the real part of the index of refraction changes by less than a factor of two. The quantity, $(n-1)^2$, is more characteristic

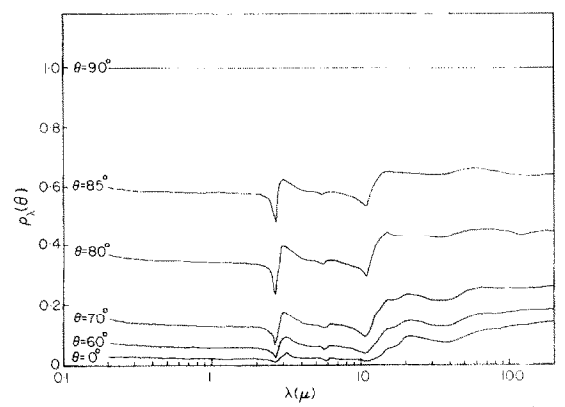

FIG. 7. Average monochromatic reflectance for various angles of incidence.

of the reflectance. From an overall energy balance standpoint, the spectral variations in the reflectance may be neglected; however, for remote sensing or spectral identification these variations are quite significant.

The spectral variation of the reflectance is presented in Fig. 7 for six different angles of incidence. The average reflectance behaves like the perpendicular component, but the spectral variation has been smoothed out somewhat for angles of incidence greater than zero. The

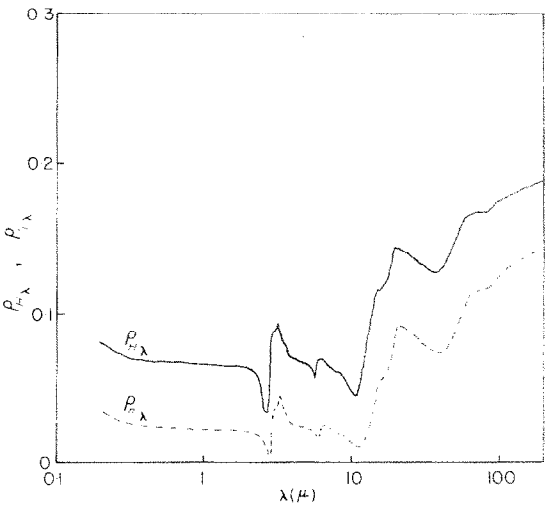

FIG. 8. Monochromatic hemispherical and normal reflectances.

monochromatic hemispherical reflectance is compared with the monochromatic normal reflectance ($\theta = 0°$) in Fig. 8 and in Table 1. For each wavelength, the hemispherical reflectance is greater than the normal reflectance; however, the spectral variation of the two reflectances is quite similar.

Total properties

We used the trapezoidal rule with 124 and 247 integration points between 0·2 and 200 μ to evaluate numerically the integrals in equations (6)–(8). The trapezoidal rule was chosen because the 124 wavelengths presented by Irvine and Pollack [9] are unequally spaced. To determine the accuracy of the numerical integra-

Table 1. *Monochromatic normal reflectance, monochromatic hemispherical reflectance*

$\lambda(\mu)$	$\rho_{n\lambda}$	$\rho_{H\lambda}$
0·20	0·03060	0·08047
0·30	0·02316	0·07050
0·40	0·02143	0·06799
0·50	0·02069	0·06689
0·60	0·02027	0·06626
0·70	0·02006	0·06594
0·80	0·01985	0·06563
0·90	0·01985	0·06563
1·00	0·01964	0·06531
1·10	0·01944	0·06499
1·20	0·01933	0·06483
1·30	0·01913	0·06451
1·40	0·01902	0·06435
1·50	0·01882	0·06403
1·60	0·01862	0·06371
1·70	0·01851	0·06355
1·80	0·01821	0·06307
1·90	0·01791	0·06259
2·00	0·01741	0·06179
2·10	0·01701	0·06114
2·20	0·01633	0·06001
2·30	0·01565	0·05887
2·40	0·01471	0·05723
2·45	0·01415	0·05624
2·50	0·01200	0·05224
2·55	0·00927	0·04658
2·60	0·00682	0·04071
2·65	0·00428	0·03324
2·70	0·00395	0·03209
2·75	0·00401	0·03245
2·80	0·01254	0·05424
2·90	0·02880	0·08216
2·95	0·03297	0·08809
3·00	0·03398	0·08851
3·10	0·03631	0·08904
3·20	0·04251	0·09497
3·30	0·03650	0·08779
3·40	0·03367	0·08432
3·50	0·03049	0·08034
3·75	0·02460	0·07252
3·83	0·02305	0·07035
4·00	0·02208	0·06894
4·50	0·02126	0·06775
4·66	0·02090	0·06721
4·80	0·02074	0·06698
5·00	0·02019	0·06615
5·26	0·01884	0·06407
5·50	0·01734	0·06168
5·80	0·01398	0·05604
6·00	0·02022	0·06695
6·05	0·02171	0·06929
6·40	0·02219	0·06923
6·50	0·02120	0·06777
7·00	0·01955	0·06525
7·50	0·01753	0·06208
8·00	0·01657	0·06052
8·50	0·01592	0·05944
9·00	0·01437	0·05679
9·50	0·01229	0·05299
10·00	0·009914	0·04835
10·50	0·008158	0·04475
11·00	0·007165	0·04351
11·50	0·009609	0·05143
12·00	0·01473	0·06349
12·50	0·01968	0·07210
13·00	0·02664	0·08309
13·50	0·03161	0·08988
14·00	0·03845	0·09866
15·00	0·05231	0·1149
16·00	0·05519	0·1155
17·50	0·06186	0·1205
18·00	0·06707	0·1250
18·50	0·05407	0·1071
19·00	0·06452	0·1177
20·00	0·08905	0·1441
25·00	0·08346	0·1389
30·00	0·07537	0·1310
33·00	0·05821	0·1114
35·00	0·07077	0·1268
40·00	0·07036	0·1275
42·00	0·07187	0·1295
50·00	0·08816	0·1469
52·00	0·05449	0·1075
60·00	0·1072	0·1645
63·00	0·06665	0·1198
75·00	0·1124	0·1674
83·00	0·1133	0·1673
100·00	0·1227	0·1749
117·00	0·1280	0·1786
150·00	0·1337	0·1831
152·00	0·1105	0·1601
200·00	0·1401	0·1887

tion, 247 integration points were used. The additional 123 data points are obtained by subdividing the original data and linearly interpolating. The total normal and total hemispherical reflectance as a function of temperature are presented in Table 2 for 124 and 247 integration points. The two sets of results exhibit excellent agreement except for low temperatures. At 300°K the reflectance values change in the second significant digit. The behavior is caused by the large variations in the monochromatic reflectance in the infrared portion of the spectrum.

Table 2. The variation of total normal reflectance, total hemispherical reflectance, Planck mean and Rosseland mean with temperature

T (°k)	ρ_n (124) pts	ρ_n (247) pts	ρ_H (124) pts	ρ_H (247) pts	κ_P, cm^{-1} (124) pts	κ_P, cm^{-1} (247) pts	κ_R, cm^{-1} (124) pts	κ_R, cm^{-1} (247) pts	$E(T)/\sigma T^4$ (124) pts	$E(T)/\sigma T^4$ (247) pts
300	0·0426	0·0441	0·0934	0·0951	1810	1810	908	919	2·00	2·01
400	0·0326	0·0334	0·0812	0·0822	1530	1530	587	602	1·86	1·86
600	0·0253	0·0257	0·0722	0·0726	1280	1280	249	258	1·78	1·78
800	0·0233	0·0235	0·0697	0·0699	1350	1340	68·0	70·8	1·77	1·77
1000	0·0223	0·0224	0·0682	0·0683	1400	1400	14·7	15·5	1·76	1·76
2000	0·0198	0·0198	0·0648	0·0648	832	831	0·0357	0·0385	1·74	1·74
3000	0·0195	0·0195	0·0647	0·0647	403	403	0·00326	0·00355	1·75	1·74
4000	0·0197	0·0197	0·0651	0·0651	214	214	0·00130	0·00142	1·76	1·75
5000	0·0200	0·0200	0·0657	0·0657	125	125	0·00092	0·00101	1·77	1·77
6000	0·0203	0·0203	0·0663	0·0663	79	79	0·00083	0·00092	1·78	1·78

The following discussion is based on the results obtained from 247 integration points. Both reflectances decrease with increasing temperature, reaching a minimum near 3000 °K and then increase slightly as the temperature is increased further. The ratio ρ_H/ρ_n increases from 2·2 at $T = 300$ °K to 3·3 at $T = 6000$ °K. The absorptance can be determined by the simple relation $\alpha = 1 - \rho$, and the emittance can be found by using Kirchhoff's law, $\epsilon(T) = \alpha(T)$. For example, the normal absorptance for a black body source at $T_s = 6000$ °K is 0·9797, while the hemispherical emittance at $T = 300$ °K is 0·9049. When the incident solar radiation is approximated by a black body at 6000 °K and the water temperature is assumed to be 300 °K, the ratio α_n/ϵ for water is 1·083.

Planck and Rosseland means

The Planck and Rosseland means were also calculated with the trapezoidal rule for 124 and 247 integration points and are included in Table 2. The two sets of results for the Planck mean are in good agreement; however, the two sets of results for the Rosseland mean exhibit considerable differences at high temperatures. Generally, these mean absorption coefficients decrease when the temperature increases. The Planck mean varies only over two orders of magnitude, while the Rosseland mean varies over six orders of magnitude. According to the Planck mean, a 1 cm thick layer of water would be classified as opaque to black body radiation at 6000 °K, but every day experience tells us that the layer is essentially transparent to solar radiation. Thus, the Planck mean fails even in the region where it should be most applicable. The Rosseland mean is more realistic. According to the Rosseland mean, a 1 cm thick layer of water would be classified as opaque to black body radiation at 300 °K and transparent to black body radiation at 6000 °K.

The quantity

$$\frac{E(T)}{\sigma T^4} = \frac{\int_0^\infty n_\lambda^2 E_{b\lambda}(T)\,\mathrm{d}\lambda}{\sigma T^4}, \tag{17}$$

might be loosely interpreted as an average of the real part of the index of refraction squared. Its magnitude is presented in Table 2 and varies only slightly with the temperature and with the number of integration points ranging from 2·01 to 1·74. In the visible region of the spectrum, the value of n is usually taken to be 1·33, or $n^2 = 1{\cdot}777$. Inspection of Table 2 reveals that $n^2 \simeq 1{\cdot}77$ at 6000 °K.

Transmittance

The monochromatic normal transmittance defined by equation (14) is presented graphically in Fig. 9 for 0·0, 1·0, 100, 1000 and 10 000 cm thick layer of water. The "0·0" cm thickness is

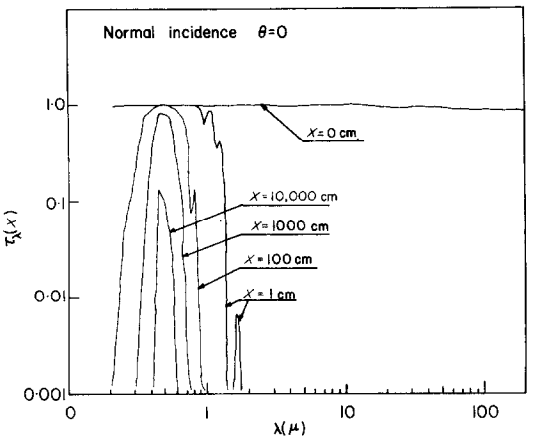

FIG. 9. Monochromatic normal transmittance at various depths into water.

to be interpreted as being on the water side of the interface and the transmittance is defined as 100 per cent. That is, that portion of the incident radiant energy which would be reflected back into the air from the interface is not taken into account [$x = 0$ in equation (14)]. Figure 9 clearly demonstrates that energy in the wavelength range between 0·3 and 0·75 μ is the only portion which penetrates to a depth of 1000 cm. The spectral energy outside this wavelength range is absorbed.

The total transmittance is calculated with the trapezoidal rule for 124 and 247 integration points and is presented in Table 3 and in Figs. 10 and 11. The 247 point integration yields lower total transmittance values than the 124 point integration. The transmittance decreases very rapidly with depth until about 200 cm when the rate of decay begins to level off. Only at excessive depths does the transmittance vary exponentially with x. For large x and the 247 point integration, the transmittance can be approximated by $\tau \simeq 0{\cdot}11\ e^{-0{\cdot}00022x}$. A similar approximation was employed by Dake and Harleman [4] for Lake Tahoe and Castle Lake data; their approximate transmittance expressions for these data are $\tau = 0{\cdot}6\ e^{-0{\cdot}0005x}$ and $\tau = 0{\cdot}6\ e^{-0{\cdot}0027x}$ respectively. A transmittance curve indicative of the data of Smith and Tyler [2] for the total normal transmittance curve indicative of Crater Lake is included in these figures. These figures would seem to indicate that the total normal transmittance of Crater Lake is better than pure water. Although Crater Lake is among the purest of natural waters and probably does exhibit a natural, maximum transmittance, it does not attenuate the incident radiant energy less than pure water. It appears to do so, however, because of the spectral region of data acquired by Smith and Tyler. They were interested mainly in the visible portion of the

Table 3. Transmittance vs depth

x (cm)	τ (124 pts)	τ (247 pts)
0	1·000	1·000
1	0·787	0·785
2	0·748	0·745
3	0·723	0·719
5	0·690	0·685
10	0·643	0·636
50	0·503	0·496
100	0·435	0·426
200	0·369	0·359
300	0·329	0·319
400	0·298	0·289
500	0·274	0·265
600	0·254	0·245
700	0·237	0·229
800	0·223	0·214
900	0·210	0·201
1000	0·199	0·190
1500	0·158	0·149
2000	0·131	0·122
2500	0·112	0·102
3000	0·0962	0·0865
3500	0·0836	0·0742
4000	0·0730	0·0642
4500	0·0640	0·0557
5000	0·0563	0·0486
6000	0·0438	0·0373
7000	0·0343	0·0288
8000	0·0269	0·0224
9000	0·0212	0·0175
10 000	0·0168	0·0137
15 000	0·00532	0·00419
20 000	0·00176	0·00134
25 000	0·00060	0·00044
50 000	0·00003	0·00002

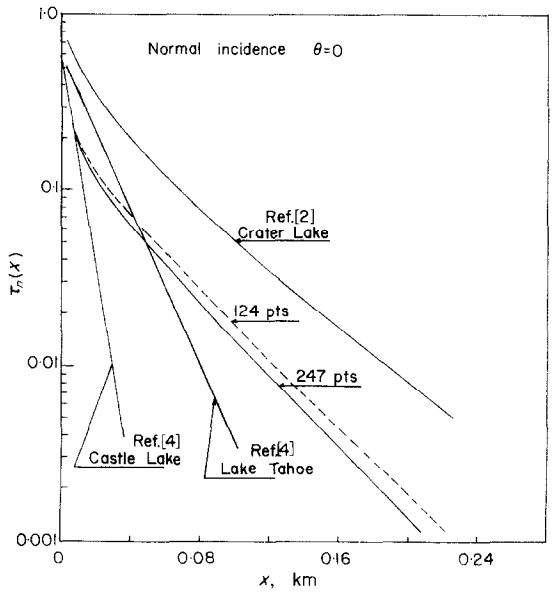

FIG. 10. Total normal transmittance as a function of depth.

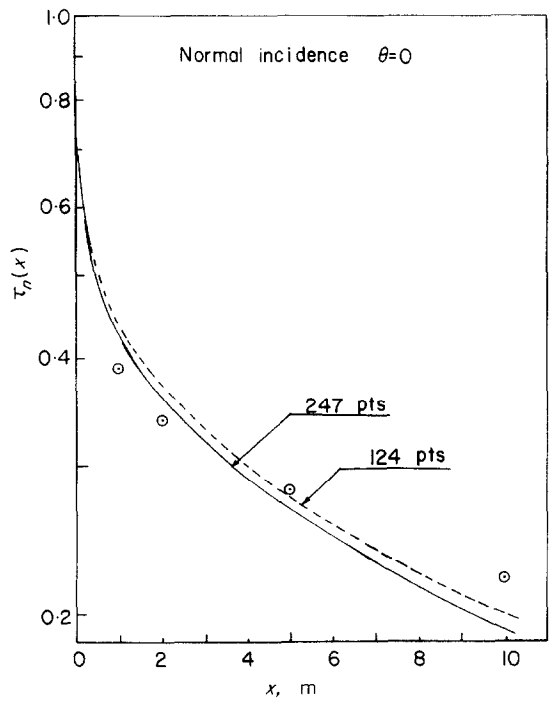

FIG. 11. Total normal transmittance as a function of depth: included are data points (⊙) from Sverdrup, Johnson and Fleming.

spectrum (0·350–0·750 μ), and as can be seen from Fig. 4, the absorption coefficient is minimum for this portion of the spectrum. The data presented in this paper consider the incident energy as coming from a black body at 6000 °K which differs from that actually received on the surface of natural waters. It covers a wider portion of the electromagnetic spectrum and thus includes regions of much less efficient transmission. Figure 11 is an expanded scale version of Fig. 10 and is presented to illustrate two points: (1) the differences between the 124 and 247 point integrations and (2) the "near-surface" effects. Data points presented by Sverdrup *et al.* [18] for sea water are included in the figure.

REFERENCES

1. C. R. GOLDMAN and R. C. CARTER, An investigation by rapid carbon-14 bioassay of factors affecting the cultural eutrophication of Lake Tahoe, California–Nevada, *J. Wat. Pollut. Control Fed.* **40**, 1044 (1965).
2. R. C. SMITH and J. E. TYLER, Optical properties of natural water, *J. Opt. Soc. Am.* **57**(5), 589 (1967).
3. N. OGURA and T. HANYA, Ultraviolet absorptance as an index of the pollution of seawater, *J. Wat. Pollut. Control Fed.* **40**, 464 (1968).
4. J. M. K. DAKE and D. R. F. HARLEMAN, Thermal stratification in lakes: analytical and laboratory studies, *Water Res. Res.* **5**(2), 484 (1969).
5. D. F. WESTLAKE, A model for quantitative studies of photosynthesis by higher plants in streams, *Int. J. Air Wat. Pollut.* **10**, 883 (1966).
6. J. R. VAN LOPIK, G. S. RAMBIE and A. E. PRESSMAN, Pollution surveillance by noncontact infrared techniques, *J. Wat. Pollut. Control Fed.* **40**, 425 (1968).
7. L. W. HOM, Remote sensing of water pollution, *J. Wat. Pollut. Control Fed.* **40**, 1728 (1968).
8. F. B. SILVESTRO, Remote sensing analysis of water quality, *J. Wat. Pollut. Control Fed.* **42**, 553 (1970).
9. W. M. IRVINE and J. B. POLLACK, Infrared optical properties of water and ice spheres, *Icarus* **8**, 324–360 (1968).
10. P. W. DAVIS, *A Bibliography of Certain Optical Properties of Liquid in the Infrared Region (1–2000 microns)*, NRL Bibl. 25 (1965).
11. V. M. ZOLOTAREV, B. A. MIKHAYLOV, L. I. ALPEROVICH and S. I. POPOV, Dispersion and absorption of liquid water in the infrared and radio regions of the spectrum, *Optika Spektrosk.* **27**(5), 430–32 (1969).
12. B. A. MIKHAYLOV and V. M. ZOLOTAREV, Emissivity of liquid water, *Atmosph. Oceanic Phys.* **6**(1), 96 (1970).
13. H. A. HYATT, Emission, reflection and absorption of microwaves at a smooth air–water interface, *J. Quant. Spectrosc. Radiat. Transfer* **10**, 217–247 (1970).

14. J. E. TYLER and R. C. SMITH, *Measurements of Spectral Irradiance Underwater*. Gordon & Breach Science Publishers (1970).
15. E. M. SPARROW and R. D. CESS, *Radiation Heat Transfer*. Brooks & Cole, Belmont, California (1966).
16. F. KREITH, *Radiation Heat Transfer for Spacecraft and Solar Power Plant Design*. International Textbook, Scranton, Penn. (1962)
17. L. D. WINIARSKI and K. V. BYRAM, Reflective cooling ponds, ASME Publ. No. 70-WA/PWR-4 (Dec. 1970).
18. H. U. SVERDRUP, M. W. JOHNSON and R. H. FLEMING, *The Oceans, Their Physics, Chemistry, and General Biology*. Prentice-Hall, Englewood Cliffs, N. J. (1942).

PROPRIETES DE RAYONNEMENT THERMIQUE D'UN INTERFACE LISSE AIR-EAU

Résumé—On a calculé les propriétés de rayonnement thermique d'un interface air-eau en supposant l'interface lisse et l'eau à une température uniforme. Ont été évalués la réflectance hémisphérique monochromatique et la réflectance totale normale, la transmittance monochromatique et la transmittance totale normale, les coefficients moyens d'absorption de Planck et Rosseland. Le domaine de longueur d'onde est compris entre 0,2 et 200 μ. D'autres propriétés de rayonnement thermique telles que l'émittance et l'absorptance ont été reliées aux propriétés déjà mentionnées et une comparaison avec des résultats connus montre un accord favorable. L'utilisation de ces propriétés dans le domaine d'action lointaine et de bilan d'énergie global rend les résultats essentiels pour identifier la région la plus active du spectre et pour expliquer quelques uns des processus naturels où le transfert par rayonnement joue un rôle important.

WÄRMESTRAHLUNGSEIGENSCHAFTEN EINER GLATTEN LUFT-WASSER-GRENZFLÄCHE

Zusammenfassung—Die Wärmestrahlungseigenschaften einer Luft-Wasser-Grenzfläche wurden berechnet unter der Annahme, daß die Grenzfläche eben ist und daß das Wasser gleichförmige Temperatur besitzt. Es wurden ausgewertet: monochromatische Reflexion in den Halbraum und die Gesamtreflexion normal zur Trennfläche, die monochromatische Durchlässigkeit und die gesamte Durchlässigkeit normal zur Trennfläche, die mittleren Plankschen und Rosslandschen Absorptionskoeffizienten. Der Wellenlängenbereich bei der Berechnung lag zwischen 0,2 and 200μ. Andere Wärmestrahlungseigenschaften wie Emission und Absorption wurden auf die obigen Eigenschaften bezogen. Ein Vergleich mit anderen Ergebnissen liefert sehr gute Übereinstimmung. Der Gebrauch dieser Eigenschaften in wenig naheliegenden Bereichen und das globale Energiegleichgewicht machen diese Daten wesentlich für das Bestimmen des wirksamsten Spektralbereiches und für die Erklärung einiger in der Natur vorkommender Prozesse, bei denen die Wärmestrahlung eine wichtige Rolle spielt.

ТЕРМОРАДИАЦИОННЫЕ ХАРАКТЕРИСТИКР ГЛАДКОЙ ПОВЕРХНОСТИ ИАЗДЕЛА ВОЗДУХ–ВОДА

Аннотация—Рассчитаны терморадиационные характеристики поверхности раздела вода–воздух, причем поверхность суиталась гладкой, а распределение температуры воды равномерным. Найдены численные значения монохроматического коэффициента отражения полусферы и общего нормального коэффициента отражения, монохроматического коэффициента пропускания и общей нормальной проницаемости, средних коэффициентов поглощения Планка и Росселанда. Расчеты проведены для длин волн от 0,2 до 200 мкм. Другие терморадиационные свойства, такие как коэффициенты поглощения и испускания, связывались с указанными характеристиками. Сравнение с имеющимися данными показало хорошее соответствие. Применение этих характеристик для дистанционного детектирования и расчета глобального баланса энергии делает эти данные существенными для определения наиболее эффективной области спектра и для объяснения некоторых естественных процессов, в которых лучистый теплообмен играет важную роль.